Impact of Mechanical and Thermal Cycles at Different Operating Conditions on the ITER Toroidal Field Coil Conductor Performance

M. Breschi[1], L. Cavallucci[1], V. Tronza[2], N. Mitchell[2], P. Bruzzone[3], K. Sedlak[3]

[1]DEI, Department of Electrical, Electronic and Information Engineering, University of Bologna, Italy

[2]ITER Organization, Route de Vinon-sur-Verdon, CS 90 046, 13067 St. Paul Lez Durance Cedex, France

[3]Ecole Polytechnique Federale de Lausanne (EPFL), Swiss Plasma Center (SPC), Villigen PSI CH5232, Switzerland

_____

Abstract

The impact of electromagnetic (EM) and thermal cyclic loading (referred as warm-up-cool-down - WUCD) on the Nb_3Sn Cable in Conduit Conductors for the toroidal field magnets of the ITER tokamak should be carefully assessed for the proper operation of the machine. The experience gained during the production phases of the TF conductors revealed that a degradation occurs when thermal and electromagnetic cyclic loading is applied at the nominal operating conditions of 10.78 T and 68 kA. Since at the beginning of the tokamak operation the nominal conditions will not be achieved, it is worth investigating to what extent lower electromagnetic loads affect the conductor performance, and the threshold of electromagnetic load that triggers the warm-up-cool-down degradation. The aim of this investigation is to identify critical levels which determine the onset of this degradation, both in terms of thermal and electromagnetic cycles, and to study the performance of strands from different suppliers.

For this assessment, a set of conductor samples were manufactured including all types of strands to be used in the TF coils of the ITER machine. These samples were subjected to a set of electromagnetic and thermal cycles representing in a realistic way the actual operation of the conductors in the ITER machine. The tests were performed in the SULTAN facility of the Swiss Plasma Center at working conditions ranging from 5.4 T -

34 kA to 10.78 T - 68 kA. This work presents the results obtained in these tests in terms of current sharing temperature (T_{cs}), effective strain, rate of degradation at different working conditions and their implications for the prospected conductor performance in the machine.

Introduction

The electromagnetic (EM) and thermal cycles can have a significant impact on the performance of Nb$_3$Sn Cable in Conduit Conductors (CICCs) for fusion magnets [1] – [3]. Given the intrinsic brittleness and the strain sensitive electromechanical behaviour of Nb$_3$Sn, the scientific community has devoted intense efforts at investigating the effects of strain on both Nb$_3$Sn wires and conductors. These studies have pointed out the effects of bending and longitudinal strain on Nb$_3$Sn wires [4] – [9] as well as the impact of cyclic loading on Nb$_3$Sn conductor performance. Several possible sources of a performance modification with cyclic loading have been identified, such as filament ruptures [10] – [12] and modifications of the strain distribution with cyclic loading [13], [14].

During both the qualification and production phases of the toroidal field (TF) conductors [15], [16], experimental tests revealed that, at the nominal working conditions of the TF coils (10.78 T, 68 kA), the performance of many samples degrades with EM cycling loading [15]. This cyclic loading consists of numerous cycles of the transport current from zero to the nominal value and then down to zero. In an additional thermal cycle, commonly referred to as warm-up-cool-down (WUCD), the samples are warmed up to room temperature and then cooled down to supercritical helium temperature. This procedure, which will necessarily be applied during the operation of the machine, may further degrade the conductor performance in terms of current sharing temperature and critical current [16]. In the usual conductor tests performed in the SULTAN facility for the qualification and production phases of the ITER TF conductors, only one thermal cycle was performed, at the end of the electromagnetic cyclic loading [17]. In a dedicated experiment in the SULTAN facility, only one of two identical conductors was subjected to 30 thermal cycles to liquid nitrogen temperature [18]. This thermal cyclic loading,

differently from the usual acceptance tests, was performed prior to the electromagnetic cyclic loading. In this experiment, the thermal cycles did not affect the degradation of the conductor, which even exhibited a slightly better performance than the one not subjected to thermal cycles. The experimental results indicated that the phase of the conductor life in which the thermal cycle is applied plays an important role on its impact on the conductor performance.

Further experimental investigations on the impact of thermal cycles were performed in the tests of the so-called TF Insert [19], a 45 m long single-layer solenoid wound with the ITER TF conductor, tested in 2016 in the CSMC facility [20] of the National Institute of Quantum and Radiological Science and Technology (QST), Naka, Japan. These investigations confirmed that the impact of the thermal cycles depends on the phase of the experimental campaign at which it is applied. It was shown that the impact of thermal cycles on the conductor performance in the curved configuration of the single layer solenoid was slightly less than that found on the straight conductor samples in SULTAN [21].

The tests of the TF Insert were performed on only one of the TF conductor types which will be used in the actual machine, along with others provided by 7 different manufacturers worldwide. Due to obvious technical and economic reasons it was not possible to manufacture one insert coil for every conductor type. It is therefore of importance to study the impact of electromagnetic and thermal cycles on all conductor types. On top of that, it should be noted that at the start of the tokamak machine operation, the TF coils will not be operated at their nominal conditions. It is therefore of relevance for the machine operation to study the extent of performance degradation in the TF conductors at magnetic field and transport currents levels below the nominal value. It is in particular important to establish at which level of the Lorentz force the onset of degradation occurs and the dependence of the rate of degradation on the working conditions of the conductor.

To this purpose, in a dedicated experimental campaign started in 2018, new SULTAN samples were prepared and tested with a sequence of EM cycles and WUCDs more representative of the real conductor life in the machine than was ever done in previous test campaigns of the TF model coil [22], TF Insert [19] and straight *production* conductor samples [16]. The samples prepared are representative of all the conductor types to be used

in the ITER TF coils. The tests were performed at different, gradually increasing levels of background DC field and transport current, starting from an initial value of the Lorentz force set to one fourth of the nominal one. The WUCDs were performed at different stages of the test campaign, and up to different temperatures (80 K and 300 K), in order to compare their impact on conductor performance. It should be noted that the thermal cycles are time consuming, since each WUCD to 80 K takes one day, while a WUCD to 300 K takes 3 days.

Since the samples were manufactured with conductors cut from the same unit lengths used to prepare the production conductor samples, a comparison with previous tests is possible, in order to study the impact of different sequences of EM and thermal cycles. It should be noted however, that in the previous SULTAN test campaigns of the TF *qualification* [15] and *production* conductors [16] the experimental runs end with an intentional quench initiation in the sample, followed by a fast current discharge. In the experimental campaign described here, instead, these quenches were avoided. Since it was observed that these fast current discharges slightly enhance the T_{cs} degradation [23], this difference could have some impact on the direct comparison between these two experimental campaigns.

In this work, the evolution of the current sharing temperature (T_{cs}) of these recent samples is reported, analysing the effects of EM cyclic loading and WUCDs on the performance at the non-nominal working conditions mentioned above. All samples are characterized by studying the evolution of effective strain and *n*-value with cyclic loading. A simple model of degradation based on the calculation of the intact filament area remaining after the possible breakage of brittle Nb_3Sn filaments caused by EM cycles and WUCDs is applied to compare the performance of all tested conductors.

1. Description of the test campaign

As already presented in [15] and [24, 25] for the previous test campaigns on the TF conductors, a pair of about 2.4 m long Cable in Conduit Conductors (CICC), commonly named left and right leg, are introduced in the bore of a magnetic system of the SULTAN facility. The background DC field is generated by 6 pairs of split solenoids which allow reaching a peak background field up to 10.8 T. The length of the peak field region

(indicated here as High Field Zone, HFZ) is 450 mm at 1% homogeneity. Since the field is not homogeneous along the conductor length, a non-uniform Lorentz force is applied to the length of the cable; some possible effects of this non-uniformity were investigated in [26]. The left and right conductor legs are fixed vertically in the bore of the magnet system and connected at the bottom by means of a solder filled joint usually referred to as the bottom joint. The two conductors are cooled by supercritical helium flowing in vertical direction from the bottom to the top of the cable.

The cable electro-thermal characteristics is measured through temperature probes and voltage taps attached to the conductor jacket. The instrumentation adopted during the TFIOXX campaign is sketched in figure 1. The two sets of temperature sensors T1 and T2 are located on the left and right leg respectively, 400 mm upstream the HFZ, whereas the two sets of temperature sensors named T3 and T4 are located 400 mm downstream the HFZ on the left and right leg respectively. Each set is composed of four temperature sensors located at a 90° angular distance. As an example, the T2 set is composed by the sensors named T21, T22, T23 and T24. The voltage sensor sets VH1 and VH2 are located on the left and right leg respectively, at a distance of 225 mm upstream the HFZ, while the two sets VH3 and VH4 are located 225 mm downstream the HFZ. Each set consists of six voltage taps mounted at a 60° angular distance, so as to measure the average voltage of the cable conduit [27].

During the test campaign analysed here, a set of five samples, named TFIO1, TFIO2, TFIO3, TFIO4 and TFIO5 (generally referred to as TFIOXX) were tested at the working conditions of 5.4 T and 34 kA, corresponding to 1/4 of the nominal Lorentz force, 7.6 T and 48 kA, corresponding to 1/2 of the nominal Lorentz force, 8.6 T and 54 kA, corresponding to 2/3 of the nominal Lorentz force, 9.7 T and 61 kA, corresponding to 4/5 of the nominal Lorentz force, and finally to the nominal working conditions of the ITER TF magnets, i.e. 10.78 T and 68 kA. Each sample consists of two conductors based on strands from different manufacturers; the strands were made with bronze process for the TFIO1, TFIO2 and TFIO3 samples and with the internal tin process for TFIO4 and TFIO5.

An additional sample, named TFIO8, was used in order to retest two production conductors that were previously subjected to the usual test campaign adopted in the production phase. This sample includes one conductor leg previously tested in the

SULTAN sample named TFEU8, and another conductor leg previously tested in the SULTAN sample named TFEU12.

The test procedure generally consists of a set of T_{cs} runs performed at the beginning of the test campaign and then after a given number of thermal and electromagnetic cycles at the working conditions mentioned above. As an example, a sketch of the test campaign for the TFIO1 sample is presented in figure 2.

A summary of the number of EM and WUCD cycles performed on each conductor and the corresponding working conditions is reported in table 1.

In the case of TFIO1 case, a total amount of 620 EM cycles were performed during the whole test campaign. The first 140 cycles were performed at 34 kA - 5.4 T background DC field. During these first EM cycles, 3 WUCD*s* up to 80 K and 3 WUCD*s* up to 300 K were also performed. A total amount of 120 EM cycles were planned at each of the following working conditions, with increasing values of the background magnetic field and transport current. During the tests at each working condition, 2 WUCD*s* to 80 K and 3 WUCD*s* to room temperature were also performed. In addition to that, between the tests at a given working condition and those at the following one, a further WUCD at 80 K was performed.

Two exceptions to this scheme were applied to the tests performed at 8.6 T and 10.78 T. During the runs at 8.6 T, a further WUCD at 300 K was performed due to a leak in the sample, while during the runs at 10.78 T only one WUCD up to 300 K was performed instead of two. After the EM cycle #620, corresponding to the last cycle at 10.78 T, a further T_{cs} run was performed to test the sample at 7.6 T and 48 kA, so as to compare the results with those previously found at the same conditions.

The TFIO2 conductor was subjected to a lower number of EM cycles, 260 in total. In particular 60 EM cycles were performed at 5.4 T – 34 kA, with 2 WUCD*s* at 300 K. After the EM cycle #260, four runs are performed at 9.7 T - 61 kA, 8.6 T - 54 kA, 7.6 T - 48 kA and 5.4 T - 34 kA. These runs are commonly referred to as unloading runs and were performed to study the extent of the irreversibility of the conductor degradation.

For the TFIO3 conductor, a total amount of 210 EM cycles were performed. This conductor was not tested at nominal conditions: after the EM cycle #210, the last one at 9.7 T – 61 kA, three T_{cs} runs were performed to study the conductor performance during

the unloading, at 8.6 T, 7.6 T and 5.4 T. The same test program applied for the TFIO3 was also followed for the TFIO4 and the TFIO5 conductors.

Two additional samples were further analysed at the end of the test campaign. The tests of the TFIO2 sample were extended with additional 675 EM cycles and 2 WUCDs. The tests of the TFIO8 conductor, as already mentioned, consist of a retest of two previously tested conductors. The test campaigns were aimed at studying the conductor performance for an extended test. In particular, 60 EM cycles at nominal operating conditions were applied, with 2 additional WUCDs to room temperature.

2. Evolution of the Current Sharing Temperature

The current sharing temperature is the signature of the DC conductor performance and is the main result of the test campaign of the TFIOXX conductors in SULTAN. The T_{cs} is derived from the measured E-T curves, as the temperature corresponding to a critical electric field of 10 µV/m. The standardized procedure to retrieve this value is explained in detail in [27].

The E-T characteristics of the conductors change during the tests, due to the EM cyclic loading and thermal cycles. Correspondingly, the T_{cs} evolves during the test campaign.

The T_{cs} evolution during the test campaign is compared in figure 3 for all TFIOXX conductors. Since the TFIO1 conductor was subjected to a greater number of EM cycles than the others, to allow a direct comparison two different x-axes are used, one corresponding to the EM cycles in the TFIO1 and another one for the TFIO2, TFIO3, TFIO4 and TFIO5. As expected, the current sharing temperature is higher at lower values of the transport current and background magnetic field and decreases as the working conditions become more severe during the test campaign.

In figure 4, the T_{cs} values of the TFIOXX conductors are reported for the first cycle, the last cycle and the unloading cycles corresponding to all working conditions. At the working conditions of 5.4 T, 34 kA, the bronze type conductors (TFIO1, TFIO2 and TFIO3) exhibit a T_{cs} of about 11.6 K; a slightly higher average value of T_{cs} is found for the internal tin conductors (TFIO4, TFIO5), with current sharing temperatures of about 11.8 K.

At this working condition, the electromagnetic load does not degrade the conductor performance. The internal tin conductors even exhibit a slight increase of performance, by about 0.1 K for the TFIO4 and 0.2 K for the TFIO5.

At the working conditions of 7.6 T, 48 kA, the internal tin conductors still exhibit slightly higher T_{cs} values than the bronze ones. Slight drops of T_{cs} can be noticed on most conductors; the two legs of TFIO3 exhibit the most stable performance.

The gradual degradation of performance proceeds for most conductors at 8.6 T and 54 kA, as shown in figure 4(c). The greatest drops of T_{cs} (0.2 K) are found for the TFIO1 and TFIO2, while the right leg of TFIO3 does not exhibit and performance drop.

At 9.7 T, 61 kA the T_{cs} difference between internal tin and bronze conductors increases. At the first cycle in this working condition, the T_{cs} of the internal tin conductors is around 7.8 K for all conductors; for the bronze conductors it is in the range from 7.2 K to 7.5 K (see figure 4(d)). The degradation with cycling loading in this working condition is in the range 0.1 K - 0.2 K for all conductors.

At the nominal working conditions of 10.78 T and 68 kA, only the TFIO1 and TFIO2 were tested. In the passage from the working conditions at 9.7 T, 61 kA to 10.78 T, 68 kA, the TFIO1 and TFIO2 sample behave differently. In both cases, between these two working conditions one WUCD to 80 K is performed. The impact of this WUCD is more severe on the performance of the TFIO1 conductors than on that of the TFIO2 conductors. The T_{cs} variations from 9.7 T, 61 kA to 10.78 T, 68 kA are 1.2 K and 1.3 K for the two conductors of TFIO1, and 0.9 K for both legs of TFIO2. This difference cannot be attributed to a difference in the strands, which are the same for the two samples. The different impact of the WUCD can probably be attributed to the greater number of EM and thermal cycles to which the TFIO1 conductor had previously been subjected. The difference in the number of cycles between these two samples is significant: a total number of 500 EM cycles and 26 WUCDs for TFIO1 versus 180 EM cycles and 9 WUCDs for TFIO2 (see table 1).

After the last run at the final working conditions, several runs were performed decreasing the electromagnetic (EM) load. The T_{cs} values for these unloading runs, shown in figure 4, are useful to estimate the irreversible part of the degradation of the conductor performance. This irreversible change of performance might be due to the breakage of the

brittle Nb_3Sn filaments or to irreversible modifications of the conductor strain distribution [13].

For the TFIO1 conductor, only one unloading run at 9.7 T was performed.

Figure 4(a) shows the T_{cs} values of the unloading cycles at 5.4 T - 34 kA. Even if this working condition does not by itself degrade the conductor performance, at the end of the test campaign a significant drop of performance is observed at these conditions. For the TFIO2, the T_{cs} drops from 11.6 K (first and last cycle of the initial runs of both legs) to 11.0 K for the left leg and 11.3 K for the right leg. A lower irreversible degradation is found for the TFIO3 conductors, from 11.6 K (first and last cycle of both legs) to 11.5 K for both legs. For both internal tin conductors, the T_{cs} drops by about 0.3 K from 11.9 K of the last cycle at 5.4 T to 11.6 K for the unloading run at the same working condition. Similar results are shown in figures 4(b), 4(c) and 4(d) for the unloading runs at 7.6 T - 48 kA, 8.6 T - 54 kA and 9.7 T - 61 kA respectively.

2.1 Spread of T_{cs} values

In the standard procedure, the current sharing temperature is computed by the voltmetric method, through the average value obtained from the six voltage signals recorded on the conduit of the conductor. If the aforementioned standard procedure is applied to each voltage tap signal, a difference is found between the T_{cs} values computed from each individual voltage tap. The difference ΔT_v between the highest and lowest T_{cs} as derived from each individual voltage tap was assessed during the previous test campaigns on the TF conductors and is also computed here for comparison and to study its variation during the test campaign.

The ΔT_v is reported in figure 5 for all conductors as a function of the EM cycles. The spread generally increases during the test campaign. The results indicate that the spread increases at higher currents; this is expected since the transverse voltage between different taps at the same longitudinal position on the jacket increases with transport current. The variation of the spread during the EM and WUCD cycles at the same working conditions is instead associated to the conductor performance degradation. In general, a lower conductor n-value is associated to a broader transition and a larger ΔT_v.

3. Analysis of the rate of degradation

In order to investigate the impact of cyclic loading on the conductor performance at different working conditions, the rate of degradation was computed in two ways. In a first approach, it is computed as the difference between the first and the last T_{cs} value at a given working condition, divided by the total number of EM cycles performed at that condition. The values found with this method include the performance variations due to the WUCDs at the analysed condition. It should be noted that this definition cannot distinguish cases in which a different number of WUCD cycles were performed at each working condition, and therefore only allows a qualitative observation of the behaviours. A direct quantitative comparison is possible for the samples TFIO3, TFIO4, and TFIO5 which were subjected to the same number of EM and WUCD cycles. In a second approach, the rate of degradation is computed as the average drop due to the EM cycles only at each working condition. In this calculation, the T_{cs} variations occurring at the WUCDs are not accounted for. The results obtained are shown in figures 6(a) and 6(b) for the first and the second approach respectively.

At 5.4 T and 34 kA, most conductors exhibit no or practically negligible degradation, which is confirmed by the null or negative values of T_{cs} variation obtained for all the TFIOXX. Instead, a slight performance drop generally occurs from 7.6 T, 48 kA to 10.78 T, 68 kA. A particular case is the TFIO3 right leg, which exhibits degradation starting only from the working conditions at 9.7 T, 61 kA. The TFIO2 generally exhibits a higher degradation rate than the other conductors.

The internal tin conductors, characterized by higher T_{cs} values, exhibit a rate of degradation similar to the bronze ones, so that no remarkable differences can be observed.

In order to point out the impact of EM cycles and WUCDs on the rate of degradation, the drop of current sharing temperature was computed for each run of the TFIO1 conductor. The TFIO1 was selected for this analysis since it was subjected to a greater number of EM cycles than the other conductors. The ΔT_{cs} is shown in figure 7 for the left leg of TFIO1, as an example. The blue symbols represent the ΔT_{cs} due to individual EM cycles. The red open symbols represent the ΔT_{cs} due to WUCDs to 80 K and the red filled symbols the ΔT_{cs} due to WUCDs to room temperature. It can be noted that each WUCD cycle has in general a greater impact on T_{cs} than one EM cycle. Figure 7 shows

that all WUCDs to room temperature determine a performance drop, apart from those performed at the initial working conditions at 34 kA, 5.4 T. This is not the case for the WUCDs at 80 K, which can either decrease or increase the conductor performance, practically at all operating conditions.

Similar analyses were carried out for the other conductors, in order to compare the impact on performance of WUCD*s* to 80 K and 300 K. The performance drops due to WUCD*s* at 80 K and 300 K are collected for all conductors in figures 8 (a) and (b) respectively. For each conductor, the *average* drops due to all WUCDs performed at a given working condition have been computed. It should be recalled that no WUCD*s* at 80 K were performed for the TFIO2 at 5.4 T, 7.6 T, 8.6 T and 9.7 T. For the TFIO3, TFIO4 and TFIO5, the WUCD*s* to 300 K correspond to the change of working condition from 9.7 T to 10.78 T. Therefore, the ΔT_{cs} at these WUCD*s* is also affected by the T_{cs} variation due to the change of working conditions and cannot directly be related to their performance degradation. These data are therefore not reported in the plots.

As shown in figure 8(a), the *average* ΔT_{cs} due to WUCDs to 80 K are either positive or negative over the whole test campaign, while the *average* ΔT_{cs} due to WUCDs to 300 K is always positive, which confirms the greater impact of the WUCDs to room temperature on the conductor degradation. In particular, the TFIO2 performance degrades significantly at nominal conditions, with average drops of 54 and 92 mK for the two legs.

4. Effective Strain and *n*-value

In the standard procedure for the analysis of the ITER conductors [27], the effective strain is taken as a fitting parameter useful to describe with a simplified approach the complex strain distribution of the conductor [15, 24]. This parameter estimates the compressive strain that should be applied to an individual strand to obtain the same *E-J* characteristics as measured on the full-size conductor. Therefore, this approach neglects possible filament ruptures in the description of the cable behaviour.

In the fitting procedure applied to estimate the effective strain ε_{eff} and the *n*-value, the measured *E-T* characteristics is reproduced by integrating the electric field computed through the power law over the cable volume *V* included in the HFZ:

$$E(T) = \frac{E_0}{LA_{tot}} \int_V \left(\frac{J_{op}}{J_c\,(B,T,\varepsilon_{eff})} \right)^n dV \tag{1}$$

where E_0 is the critical electric field, L the conductor length, A_{tot} the area of the cable cross section, J_{op} the operating current density of the cable, J_c the critical current density as a function of magnetic flux density B, temperature T and effective strain ε_{eff}. The ITER parameterization of the superconductor critical surface [28] is applied to estimate J_c (B, T, ε_{eff}). It should be noted that the parameters to be used for this function differ from strand to strand, and are reported in [16].

In the procedure, only the experimental values with electric fields included in the range from 5 to 50 µV/m are considered for the fitting.

4.1. Evolution of the effective strain

The results of the effective strain are presented in figure 9 for all TFIOXX conductors. The internal tin conductors generally exhibit lower absolute values of effective strain, corresponding to the higher measured T_{cs} values. For TFIO5, the effective strain at 5.4 T - 34 kA is not reported, due to the very limited amount of data in the range 5 - 50 µV/m.

It can be noticed that the absolute value of the ε_{eff} increases at more severe working conditions. The highest absolute values of effective strain, up to 0.97 %, is found for the TFIO1 and TFIO2 conductors at the end of the test campaign, at nominal conditions.

In order to analyse the impact of the EM cycles, WUCD*s* and working conditions on the effective strain, figure 10 shows the effective strain at the first, last and unloading cycle at the same working conditions. At all working conditions, apart from 5.4 T – 34 kA, the EM cycles determine an increase of the effective strain absolute value. As an example, for the TFIO1 conductor ad 7.6 T - 48 kA, the effective strain drops from −0.77 % at the first cycle to −0.81 % for the last cycle and finally to −0.93 % at the unloading. This variation is found on all conductors and is related to the conductor degradation.

Following a simple approach [29, 30], the effective strain can be related to the thermal strain and Lorentz forces according to the following relation:

$$\varepsilon_{eff} = \varepsilon_{th} - kI_{op}B \tag{2}$$

where $\boldsymbol{\varepsilon_{th}}$ is the thermal strain contribution, $\boldsymbol{k}$ the so-called *crushing strain* coefficient, I_{op} the operating current and B the magnetic flux density. These parameters can be computed

through linear interpolation of the effective strain at the different working conditions. Three methods can be applied for the extrapolation. In the first method, the effective strain computed at the first cycle of each working condition is used for the extrapolation, thus minimizing the effect of the conductor degradation on the parameters. A second method is based on computing the coefficients considering the last cycle at each working condition. This second approach describes the conductor in a state of more advanced degradation than the previous approach. The third method estimates ε_{th} and k via interpolation of the results obtained during the unloading runs, which describe the conductor at its final state after the whole test campaign. The linear fit in Equation (2) was applied to all TFIOXX conductors; as an example, the results of the TFIO2 left leg are reported in figure 11. The thermal strain of the unloading runs is significantly greater (in absolute terms) than that obtained with the first tests at each working condition. On the other hand, the slope of the linear variation is significantly reduced at the end of the test campaign with respect to the initial values. Similar trends are confirmed for all TFIOXX conductors; the corresponding results are collected in table 2. The data reported build up a rather wide database to describe the behaviour of a TF conductors subjected to cyclic electromagnetic and thermal loading.

4.2. Evolution of the n-value

An example of the evolution of the *n*-value during the test campaign is presented in figure 12 for the TFIO3 conductor. It can be noticed that the *n*-value decreases during the test campaign over the various test conditions from 7.4 (left leg) and 6.6 (right leg) at 5.4 T, 34 kA to 4.3 (left leg) and 4.0 (right leg) at 9.7 T, 61 kA prior to the unloading. It should be noted that, since the *n*-value of the individual strands depends on the critical current [31], the variation of the *n*-value with the change of working conditions is expected. The change of *n*-value during the tests at each working condition is a more direct indicator of the conductor performance evolution during the cyclic loading.

The results obtained during the unloading runs are quite unexpected. While the T_{cs} recovers higher values during these runs, given the reduction of transport current and background field, the *n*-value keeps decreasing, with significant drops found on all conductors during the unloading runs.

In figure 13, the n-values at the first, the last and the unloading cycle at the same working conditions of all the TFIOXX conductors are shown.

The behaviour of the n-value previously described for the TFIO3 sample is found for all conductors. In particular, during the unloading runs, even if the working conditions become less severe and the T_{cs} recovers higher values (see figure 3), the n-values keep dropping quite dramatically. This determines a large difference between the n-values found during the test campaign and those obtained during the final unloading runs. As an example, at 5.4 T - 34 kA, the n-value of the TFIO4 left leg drops from 7.0 at the first EM cycle to 6.2 at the last EM cycle of the initial phase of tests, down to 3.9 at the unloading cycle.

5. Intact Filament Area

During the EM and thermal cycles, the evolution of the conductor performance is due to both the modification of the strain distribution [14], and to the rupture of some of the brittle Nb_3Sn filaments [12]. The filament ruptures occur when the tensile strain related to bending reaches sufficiently high values, which have also been investigated through direct measurements on individual filaments [32]. Given the difficulty to account simultaneously for the variation of the strain distribution and of the filaments intact area, in Section 4 the degradation has been exclusively attributed to the variation of the effective strain, a fitting parameter obtained neglecting the possible presence of broken filaments. Another possible approach is to describe the conductor performance evolution by attributing the degradation partially to the rupture of filaments; this can be obtained by computing the portion of superconducting area that still contains intact filaments.

The intact filament area is estimated through a best fitting procedure similar to the one described in Section 4 to derive the effective strain and the n-value. In this case, the following equation is adopted:

$$E(T) = \frac{E_0}{LA_{tot}} \int_V \left(\frac{J_{op}}{k \, J_c \, (B,T,\varepsilon_{eff})} \right)^n dV \qquad 3$$

where k is the ratio of the intact filament area to the total filament area. In this calculation, the two fitting parameters are k and n, while the effective strain must be set to a given value prior to the calculation. This value is computed as explained in the following.

The effective strain is assumed a function of the electromagnetic load I×B and is computed via the linear interpolation reported in Equation (2). As previously discussed, the parameters ε_{th} and k in Equation (2) can be estimated from the linear interpolation of either the first cycle, the last cycle or the unloading runs. The thermal strain ε_{th} values are taken from the interpolation of the results obtained at the first cycle. This choice allows minimizing the impact of the conductor degradation on the assessment of the thermal strain. On the other hand, the slope k is determined by interpolation of the results found for the unloading runs (see table 2). In the unloading runs, the portion of conductor degradation which is reversible can somewhat be separated from the irreversible part. Therefore, in these conditions, the parameter k allows one better assessing the impact of I×B on the effective strain of the conductor.

The ratio between the intact filament area and the total superconducting area is reported in figure 14. The final intact filament area is about 60 % of the initial one at the end of the test campaign, which is compatible with previous results on the first CS Insert coil [33]. It can be noticed that while TFIO1 and TFIO2 start degrading at operating conditions with rather low I×B, TFIO3 and TFIO5 exhibit a nearly constant value of intact filament area throughout the initial operating conditions, up to 9.7 T, 61 kA. This indicates that for the latter conductors the initial variations of current sharing temperature are essentially related to the impact of strain on the conductor performance. The overall *variation* of intact filament area during the test campaign is around 20 % for both legs of TFIO1, the left leg of TFIO2 and TFIO4. The right leg of TFIO2, the left leg of TFIO3 and both legs of TFIO5 exhibit an intermediate variation of the filament area in the order of 10 %. The right leg of TFIO3 exhibits only a 3 % variation of the intact filament area over the whole test campaign. It is worth noting that the right leg of TFIO3 is made with the conductor procured by the Russian Federation DA, which is known to be less prone to performance degradation with electromagnetic cyclic loading [16].

6. Extended Cyclic Loading Tests

This section reports the results of the retest of two conductor samples, performed after the end of the initial test campaign. The first one is the TFIO2 sample, which was subjected to additional 675 EM cycles and 2 WUCDs.

Figure 15 shows the current sharing temperature found in these extended tests. At the last EM cycle of the first test campaign of TFIO2, at 10.78 T, 68 kA, the current sharing temperatures of two legs equal 5.5 K and 5.9 K for the left and the right leg respectively. At the first cycle of the retest sample, the T_{cs} drops to 5.4 K and 5.6 K for the left and right leg respectively. It is worth noting that a thermal cycle to room temperature was performed before the retest due to the removal of the sample from the facility. At the end of the tests, after 935 total cycles and a further WUCD, the conductor exhibits T_{cs} values of 5.1 K and 5.5 K for the left and the right leg respectively.

The tests of the TFIO8 conductor essentially consist of a retest of two conductors which were previously tested in SULTAN [16]. The left leg of the TFIO8 corresponds to the right leg of sample TFEU8, while the right leg of TFIO8 corresponds to the left leg of sample TFEU12. In the previous tests, the conductors were subjected only to 1000 EM cycles, followed by 1 WUCD, which is the usual procedure applied to production conductors [16]. In the retest, the TFIO8 sample was submitted to 2 WUCDs and 60 EM cycles. The evolution of T_{cs} of TFIO8 is shown in figure 16, which also reports the results of the previously tested samples. After 1000 EM cycles, the T_{cs} of the TFEU8 right leg drops from 6.2 K to 5.8 K. After the first WUCD, the T_{cs} further drops to 5.6 K, while after the second WUCD, related to the sample removal, it reaches 5.3 K. A final value of 5.2 K is found after 60 further EM cycles. A similar drop of performance and degradation rate is observed for the TFIO8 right leg.

The results reported in figures 15 and 16 show a different behaviour of the TFIO2 and TFIO8 conductors. In particular, the TFIO8 exhibits a rapid drop of performance after the second WUCD. The T_{cs} decreases by 0.14 K in 60 EM cycles, corresponding to a degradation rate of about 2.3 mK/cyc. The results of the test extension of TFIO2 show an initial performance drop after the thermal cycle corresponding to the sample removal (at EM cycle #260), but after that the T_{cs} remains rather stable. A total drop of 0.3 K in 670 EM cycles is observed, corresponding to a degradation rate below 0.5 mK/cyc, which is four times lower than that found for TFIO8.

The different performance of these conductors can be correlated to the different types of test campaigns they were subjected to. The dramatic performance drop of the TFIO8 sample occurs after the conductors were subjected to 2 thermal cycles at the end of the

conductor life, after 1000 EM cycles at nominal conditions. The TFIO2 conductors instead, were submitted to 14 thermal cycles, as well as 260 EM cycles at low values of Lorentz force, plus the additional 675 EM cycles and 2 WUCDs of the retest at nominal conditions. The latter type of conductor solicitation is much closer to the real operating conditions in the ITER tokamak than that experienced by TFIO8.

These results give an indication that thermal and EM cycles at low Lorentz force levels, applied alternatively during the initial phase of the conductor life, can play a role in improving its performance at nominal conditions, as already pointed out in [2]. As anticipated in the introduction, since intentional quenches were induced in the production conductors at the end of the test campaign, this different behaviour could also partly be attributed to those quench events.

7. Conclusions

This work reports a comprehensive analysis of the test results concerning the impact of electromagnetic and thermal cycles at different operating conditions on the performance of the Cable in Conduit Conductors for the TF coils of the ITER magnet system. These data build up a database which could be regarded as a reference for detailed studies on conductor degradation or for the prediction of the conductor performance in the actual working conditions of the ITER machine.

The results show that the initial cyclic loading performed at 5.4 T and 34 kA does not significantly affect the performance of any type of TF conductor. In particular, the current sharing temperature does not show any remarkable drop for the bronze type conductors, and even exhibits a slight increase with for the internal tin conductors (all legs of samples TFIO4 and TFIO5). The performance drop starts at 7.6 T and 48 kA for all conductors, with the exception of TFIO3 which starts exhibiting some degradation at 8.6 T and 54 kA.

The results clearly show a different impact of electromagnetic (EM) cycles when applied at different levels of applied transverse load. In particular, the rate of conductor degradation increases with the applied transverse load. As an example, the average drop of current sharing temperature for all conductors due to 1 EM cycle is 0.5 mK at 7.6 T and 48 kA and 2.6 mK at 9.7 T, 61 kA.

Comparing the impact of EM and WUCD cycles, the WUCDs have a predominant impact on the TF conductor performance. A different effect of the WUCDs to 80 K was found with respect to those to 300 K. Comparing the *average impact* of various thermal cycles at each working condition, the WUCDs to 80 K have either a positive or negative impact on performance, while the WUCDs to 300 K always determine a performance drop, which is higher than that due to WUCDs to 80 K, especially at the end of the test campaign.

The results concerning the effective strain show that the internal tin conductors are characterized by a lower effective strain (in absolute value) than the bronze type ones. The effective strain ranges from −0.79 % to −0.50 % for the internal tin conductors whereas it is in the range from −0.97 % and −0.62 % for the bronze type ones. The effective strain exhibits quite a good linear correlation with the transverse loading force, even when computed at various phases of the conductor test campaign. This relation could allow one determining the effective strain in the conductor, and therefore the current sharing temperature, at electromagnetic loads which differ from those usually applied in the SULTAN tests, and at different phases of the conductor life in the machine.

The results obtained at the unloading runs show that the current sharing temperature recovers the values found during the previous tests at the same working condition, with a small drop related to the impact of the conductor degradation. On the opposite, a significant drop of the *n*-value is found for all conductors during the unloading runs, notwithstanding the significant reduction of the applied transverse load.

The intact area of the superconducting filaments is included between 60 % and 97 % of the initial value, which is a result in line with previous observations on the value of this parameter. It should be noted that the degradation in terms of filament fracture shows a stabilising trend. Although there is still some impact related to the effective strain, as shown in the evolution of the current sharing temperature, the mechanical damage seems to be trending to a limit at the end of the test campaign.

Acknowledgment

Disclaimer

References
[1] Devred A et al 2012 Status of ITER conductor development and production, *IEEE Trans. Appl. Supercond.*, **22**, 4804909,
[2] Mitchell N *et al* 2020 The use of Nb$_3$Sn in fusion: lessons learned from the ITER production including options for management of performance degradation *Supercond. Sci. Technol.* **33** 054007
[3] Weiss K P *et al* 2007 Systematic approach to examine the strain effect on the critical current of Nb$_3$Sn cable-in-conduit-conductors *IEEE Trans. Appl. Supercond.* **17** 1469–72
[4] Mitchell N *et al* 2013 Reversible and irreversible mechanical effects in real cable-in-conduit conductors *Supercond. Sci. Technol*. **26** 114004
[5] Kajitani H *et al* 2013 Analytical study of degradation of CIC conductor performance due to strand bending and buckling *IEEE Trans. Appl. Supercond.* **23** 6001505
[6] Mitchell N 2003 Mechanical and magnetic load effects in Nb$_3$Sn cable-in-conduit conductors *Cryogenics* **43** 255–70
[7] Schultz J H *et al* 2005 Transverse stress effects in ITER conductors *IEEE Trans. Appl. Supercond.* **15** 1371–4
[8] Nijhuis A *et al* 2009 Summary of ITER TF strand testing under axial strain, spatial periodic bending and contact stress *IEEE Trans. Appl. Supercond.* **19** 1516–20
[9] Bajas H *et al* 2010 Numerical simulation of the mechanical behaviour of ITER cable-in-conduit conductors *IEEE Trans. Appl. Supercond.* **20** 1467–70
[10] Jewell M C *et al* 2003 The influence of Nb$_3$Sn strand geometry on filament breakage under bend strain as revealed by metallography *Supercond. Sci. Technol.* **16** 1005–11
[11] Nijhuis A *et al* 2009 Systematic study on filament fracture distribution in ITER strands *IEEE Trans. Appl. Supercond.* **19** 2628–32
[12] Sanabria C *et al* 2012 Evidence that filament fracture occurs in an ITER toroidal field conductor after cyclic Lorentz force loading in SULTAN *Supercond. Sci. Technol.* **25** 075007
[13] Calzolaio C *et al* 2013 Monitoring of the Thermal Strain Distribution in CICCs During the Cyclic Loading Tests in SULTAN *IEEE Trans. Appl. Supercond.* **23** 4200404–4200404

[14] Calzolaio C and Bruzzone P L 2014 Analysis of the CICC Performance Through the Measurement of the Thermal Strain Distribution of the Nb3Sn Filaments in the Cable Cross Section *IEEE Trans. Appl. Supercond.* **3** 4802204– 4802204

[15] Breschi M *et al* 2012 Results of the TF conductor performance qualification samples for the ITER project *Supercond. Sci. Technol.* **25** 095004

[16] Breschi M *et al* 2017 Performance analysis of the toroidal field ITER production conductors *Supercond. Sci. Technol.* **30** 055007

[17] Bruzzone P L *et al* 2012 Operation and test results from the SULTAN test facility *IEEE Trans. Appl. Supercond.* **22** 9501704

[18] March S *et al* 2012 Effect of Thermal Loading on Nb_3Sn CICC Performance *IEEE Trans. Appl. Supercond.* **22** 4803604

[19] Ozeki H *et al* 2016 Manufacture and Quality Control of Insert Coil With Real ITER TF Conductor *IEEE Trans. Appl. Supercond.* **26** 4202504

[20] Ando T and Tsuji H 2001 ITER central solenoid (CS) model coil project *Teion Kogaku—J. Cryogenics Supercond. Soc. Jpn.* **36** 309

[21] Nabara Y *et al* 2012 Examination of Japanese Mass-Produced Nb_3Sn Conductors for ITER Toroidal Field Coils *IEEE Trans. Appl. Supercond.* **22** 4804804

[22] Komarek P *et al* The test facility for the ITER TF model coil *Fusion Engineering and Design* **41** 213–221

[23] Sedlak K *et al* 2021 T_{cs} degradation of ITER TF samples due to fast current discharges *Supercond. Sci. Technol.* **34**, 025004

[24] Breschi M *et al* 2011 Evaluation of effective strain and n-value of ITER TF conductor samples *IEEE Trans. Appl. Supercond.* **21** 1969–73

[25] Breschi M *et al* 2012 Error Estimation in the T_{cs} Measurement of TF Conductors in the SULTAN Facility *IEEE Trans. Appl. Supercond.* **22** 3 4805205

[26] Devred A, Jong C and Mitchell N 2012 Strain redistribution effects on current-sharing temperature measurements on straight sample of large Nb_3Sn cable-in-conduit conductors *Supercond. Sci. Technol.* 25 054009

[27] Bessette D *et al* 2010 Sensitivity analysis of T_{cs} measurement on ITER TF conductors *IEEE Trans. Appl. Supercond.* **20** 3 1488-1491

[28] Bottura L and Bordini B 2009 Jc(B, T, ε) parameterization for the ITER Nb3Sn production *IEEE Trans. Appl. Supercond.* 19 1521–4

[29] Zanino R *et al* 2003 Analysis and interpretation of the full set (2000–2002) of T_{cs} tests in conductor 1A of the ITER Central Solenoid Model Coil *Cryogenics* **43** 179–197

[30] Martovetsky N *et al* 2017 Characterization of the ITER CS conductor and projection to the ITER CS performance *Fusion Eng. Des.* **124** 1–5

[31] Taylor M J and Hampshire D P 2005 Relationship between the *n*-value and critical current in Nb_3Sn superconducting wires exhibiting intrinsic and extrinsic behaviour *Supercond. Sci. Technol.* **18** S297–S302

[32] Dylla M T et al 2016 Fracture Strength Distribution of Individual Nb3Sn Filaments *IEEE Trans. Appl. Supercond.* **26** 6001907– 6001907

[33] Mitchell N 2007 Assessment of conductor degradation in the ITER CS insert coil and implications for the ITER conductors *Supercond. Sci. Technol.* **20** 25–34

Tables

Table 1. Number of EM cycles and WUCDs at each working condition for the TFIOXX conductors

| | | 5.4 T - 34 kA | | 7.6 T - 48 kA | | 8.6 T - 54 kA | | 9.7 T - 61 kA | | 10.78 T - 68 kA | |
		EM Cycle	WUCD	EM Cycle	WUCD	EM Cycle	WUCD	EM Cycle	WUCD	EM Cycle	WUCD
Bronze	**TFIO1**	140	4 (80 K) 3 (RT)	120	3 (80 K) 3 (RT)	120	3 (80K) 4 (RT)	120	3 (80K) 3 (RT)	120	2 (80K) 1 (RT)
	TFIO2	60	3 (RT)	40	2 (RT)	40	2 (RT)	40	1 (RT) 1 (80K)	80	2 (RT) 1 (80K)
	TFIO3	60	3 (80K)	40	2 (80K)	40	1 (80K) 1 (RT)	70	/	/	/
Inter. Tin	**TFIO4**	60	3 (80K)	40	3 (80K)	40	1 (80K) 1 (RT)	70	/	/	/
	TFIO5	60	3 (80K)	40	2 (80K)	40	1 (80K) 1 (RT)	70	/	/	/

Table 2. Linear fit of the effective strain dependence on transverse load

| | | Begin Working Conditions | | End Working Conditions | | Unloading | |
		k [AT]	ε_{th} [%]	k [AT]	ε_{th} [%]	k [AT]	ε_{th} [%]
TFIO1	Left	-0.45	-0.61	-0.47	-0.64	-0.10	-0.90
	Right	-0.49	-0.54	-0.53	-0.55	-0.23	-0.76
TFIO2	Left	-0.43	-0.57	-0.49	-0.57	-0.20	-0.79
	Right	-0.41	-0.63	-0.45	-0.63	-0.28	-0.76
TFIO3	Left	-0.20	-0.70	-0.28	-0.67	-0.16	-0.75
	Right	-0.20	-0.65	-0.26	-0.62	-0.21	-0.66
TFIO4	Left	-0.42	-0.46	-0.49	-0.43 %	-0.32	-0.54 %
	Right	-0.28	-0.47	-0.22	-0.51 %	-0.17	-0.54 %
TFIO5	Left	-0.40	-0.36 %	-0.46	-0.35 %	-0.27	-0.47 %
	Right	-0.46	-0.35 %	-0.49	-0.36 %	-0.24	-0.51 %
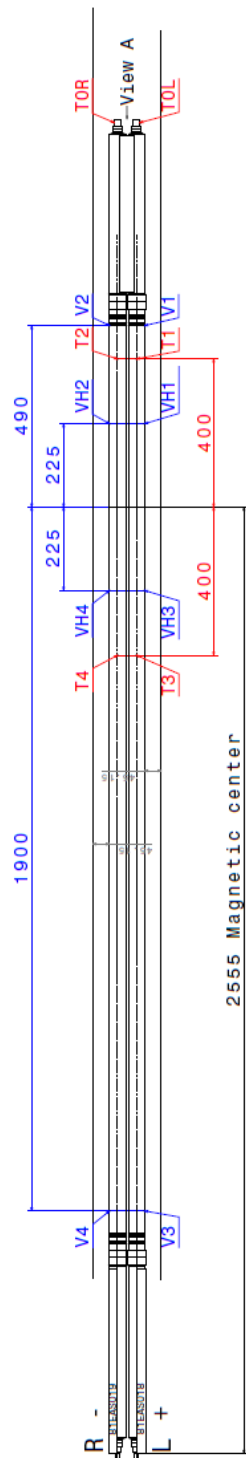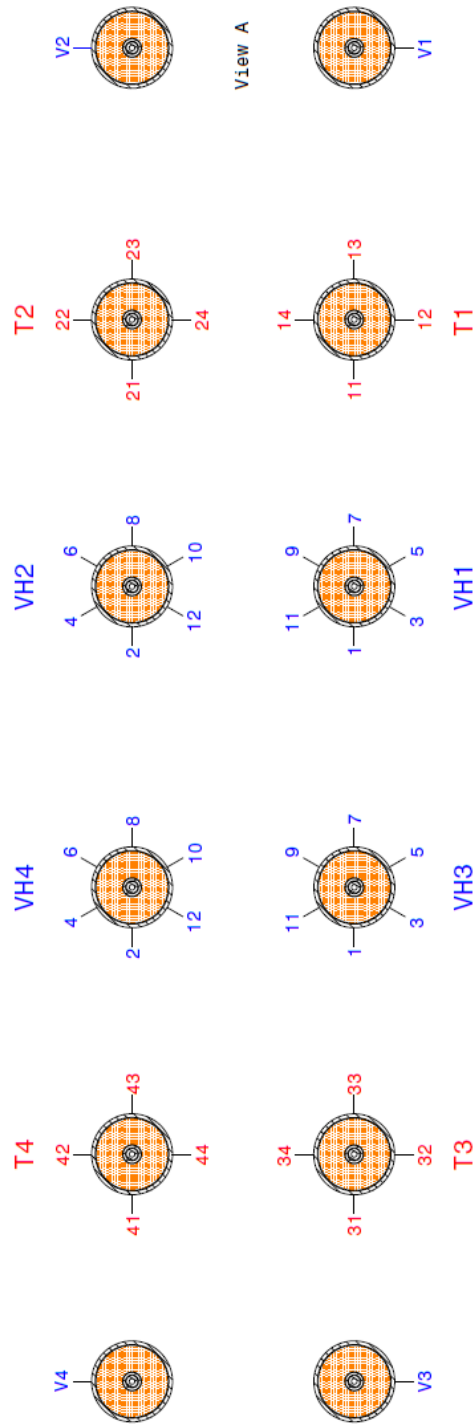
Figure 1. *Sketch of a typical SULTAN sample for the ITER TF conductors with upper terminations, bottom joint, temperature probes and voltage taps. The voltage taps crowns are located upstream (VH1 and VH2) and downstream (VH3 and VH4) of the HFZ, at* 225 mm *distance from its center. The helium inlet is at the bottom joint and the flow is upwards. The background magnetic field is directed perpendicular to the conductor axis.*
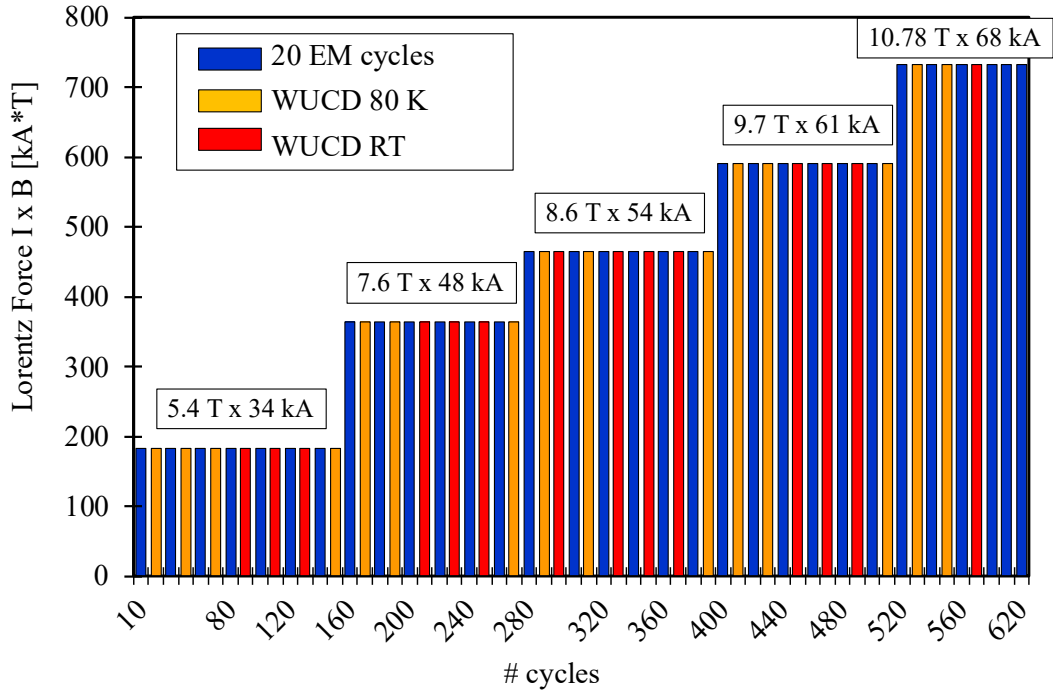
Figure 2. *Sketch of the test program of the TFIO1 conductor. The height of the bars corresponding to the WUCDs is kept the same as the neighbouring ones for the graphics, but of course there is no Lorentz force applied during the thermal cycles.*
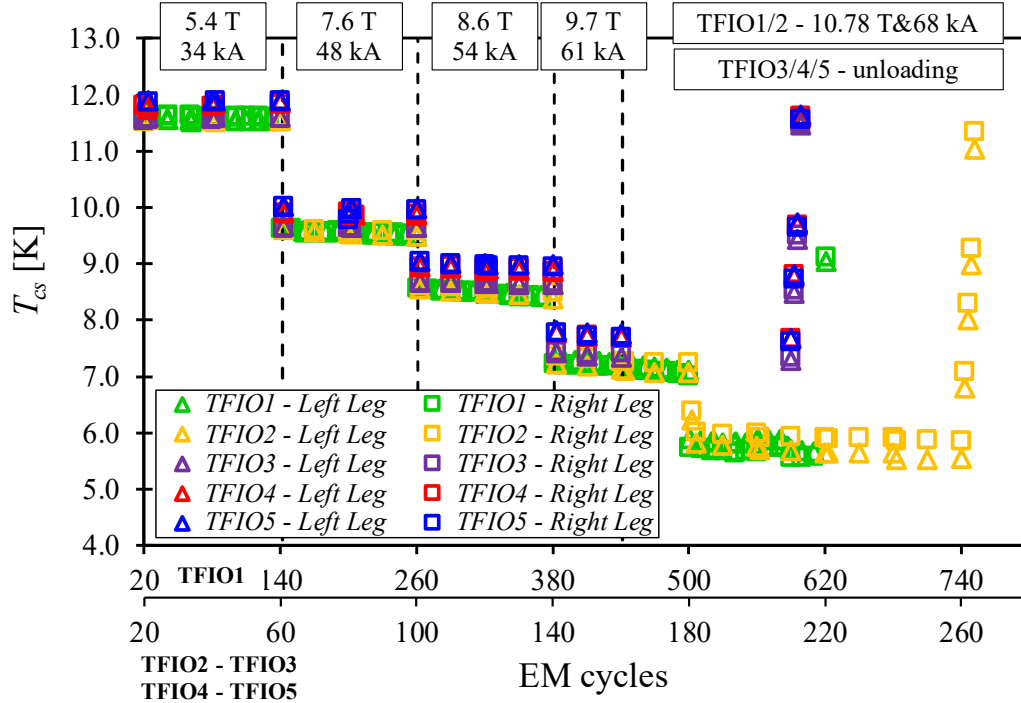
Figure 3. *Voltmetric T_{cs} of the TFIOXX conductors as a function of the number of EM cycles.*
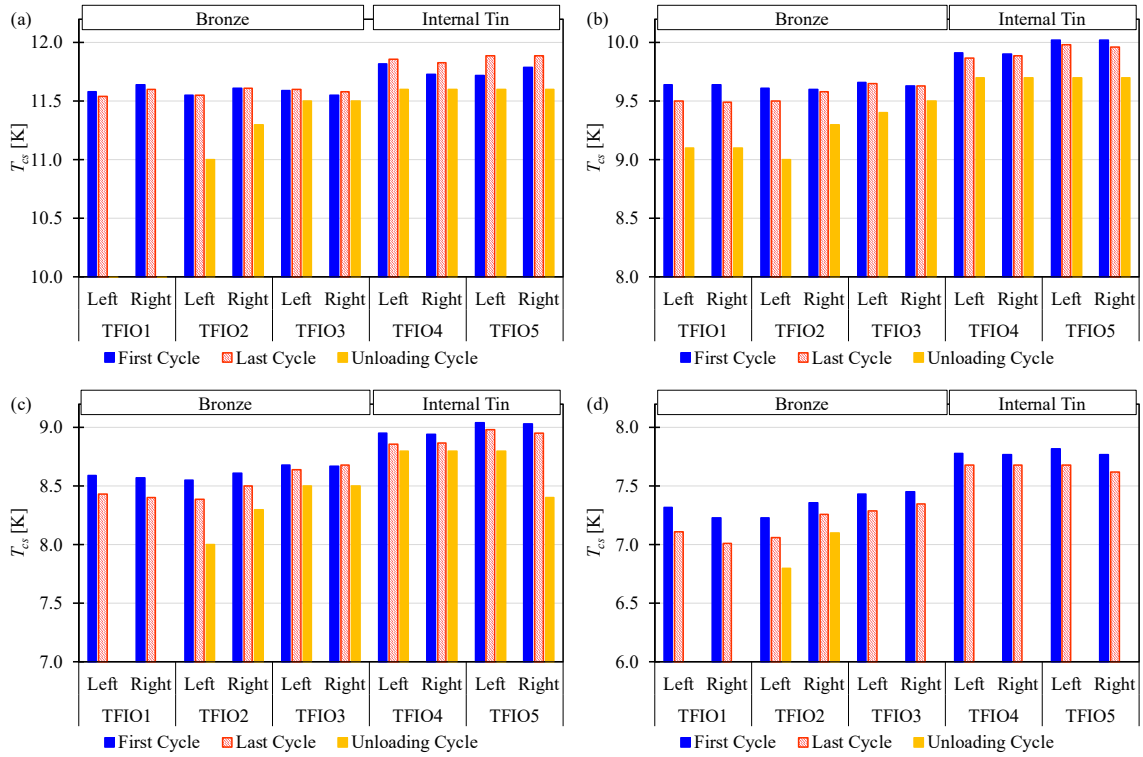
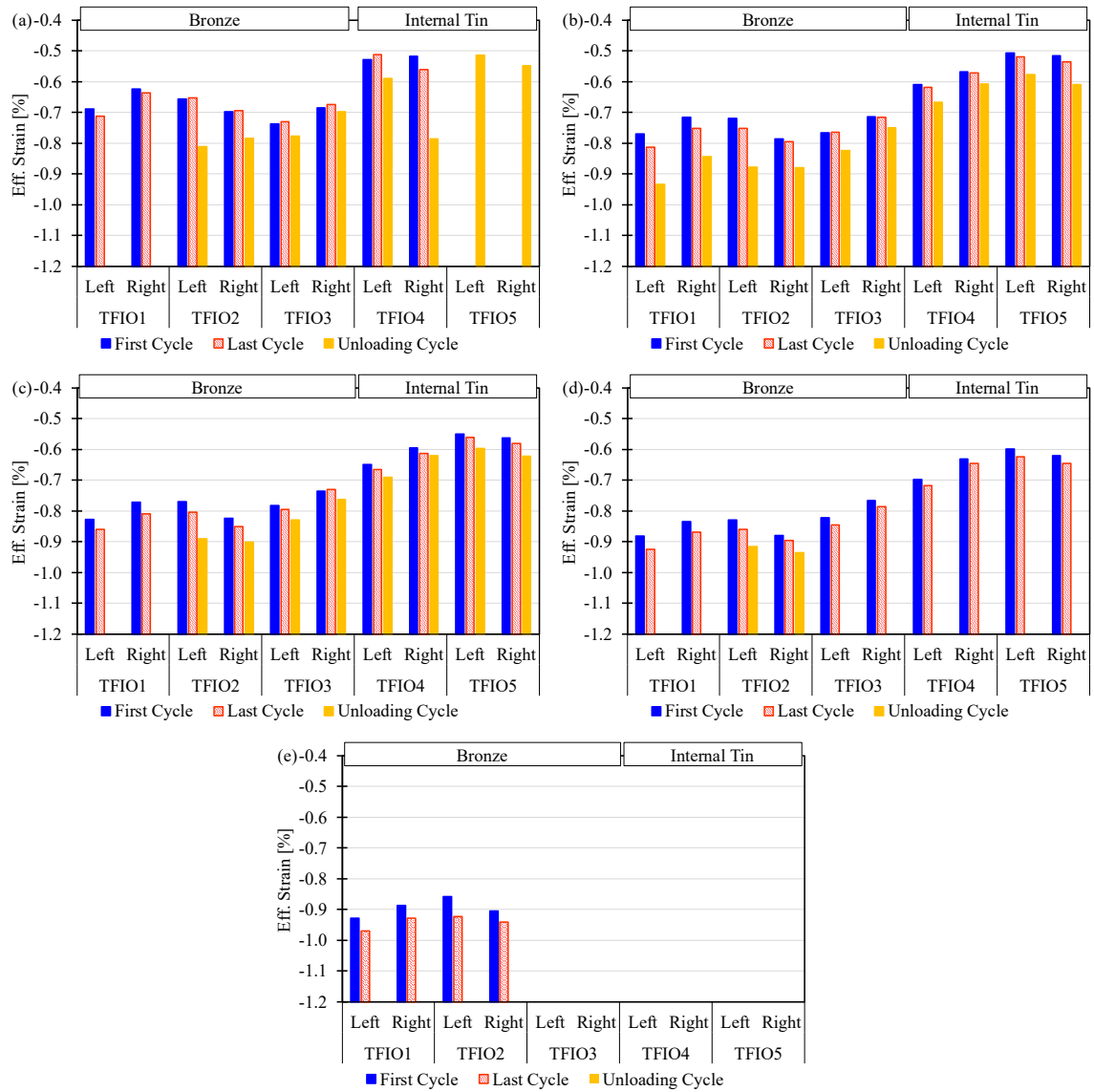Figure 4. *T_{cs} values of the TFIOXX conductors at the working conditions of (a) 5.4 T - 34 kA, (b) 7.6 T - 48 kA, (c) 8.6 T - 54 kA and (d) 9.7 T - 61 kA*
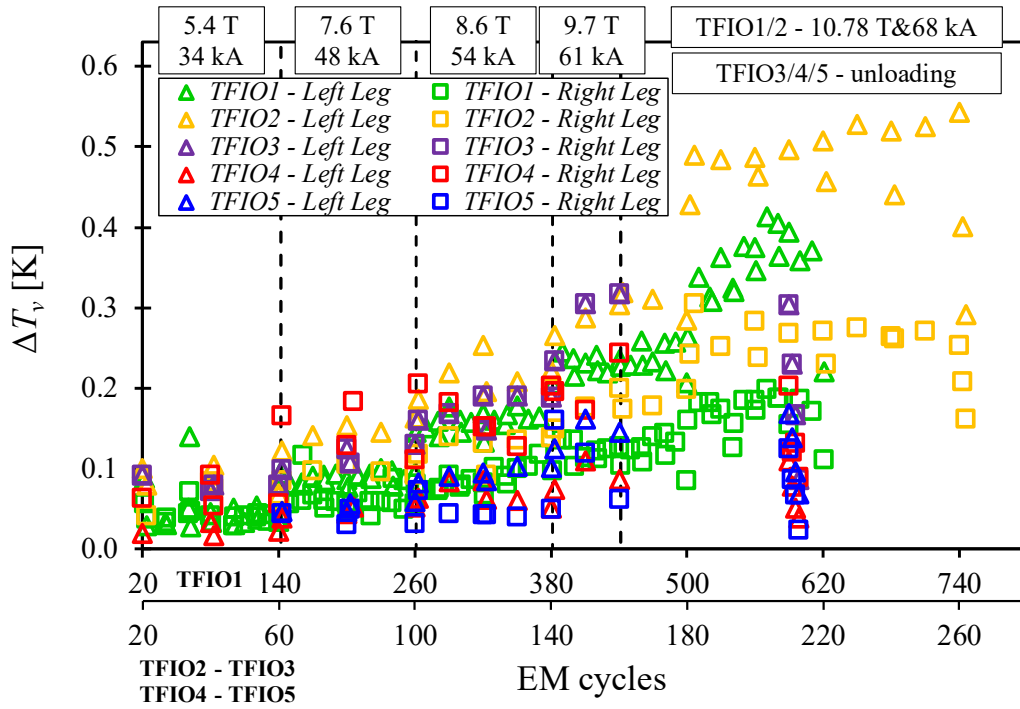
Figure 5. *Spread of T_{cs} from individual voltage taps of the TFIOXX conductors as a function of the number of EM cycles.*
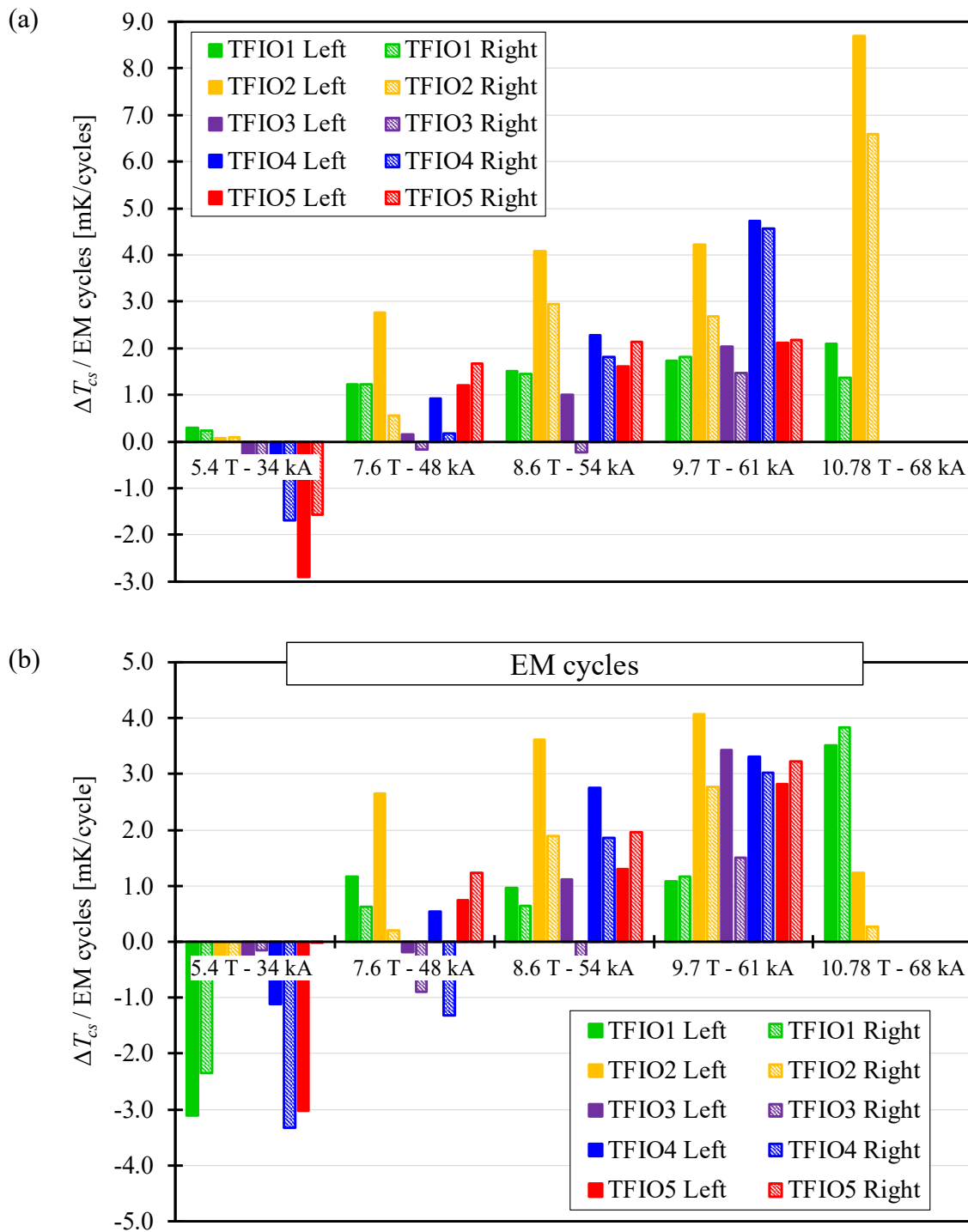
Figure 6. *Rate of degradation of the TFIOXX conductors as a function of the number of EM cycles. a) Total T_{cs} drop at each working condition divided by the number of EM cycles at the same working condition (including the effect of WUCDs) b) T_{cs} drop at each working condition only due to the EM cycles divided by the number of EM cycles at the same working condition (impact of WUCDs excluded).*
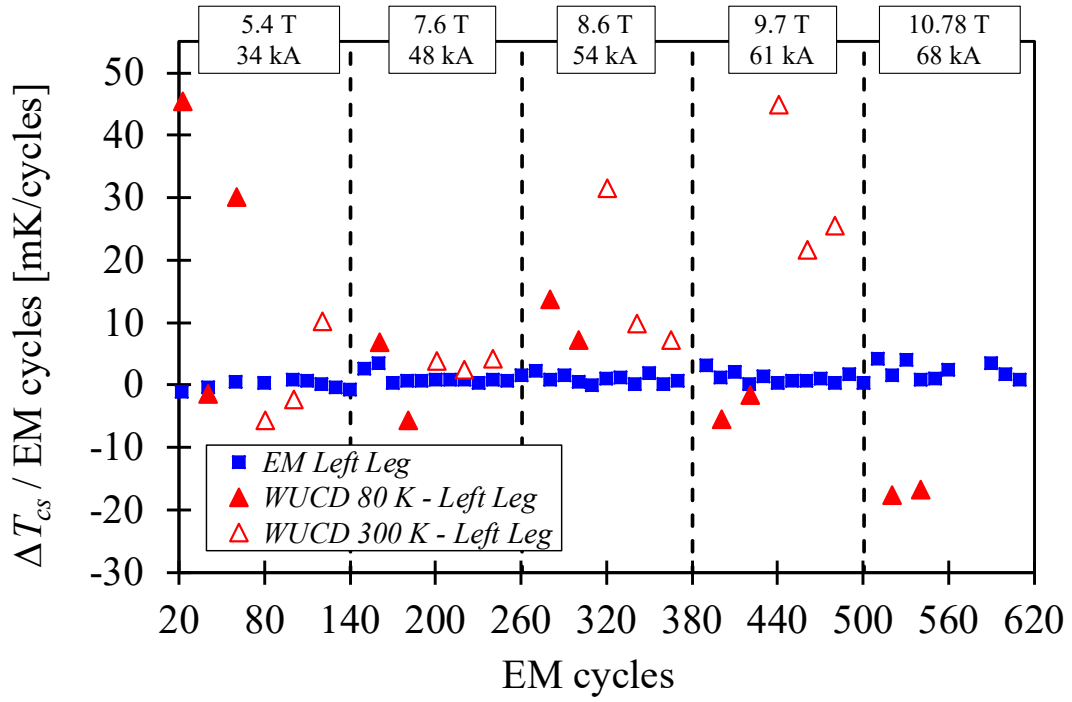
Figure 7. *Rate of degradation of the TFIO1 (a) right leg and (b) left leg as a function of the number of EM cycles.*
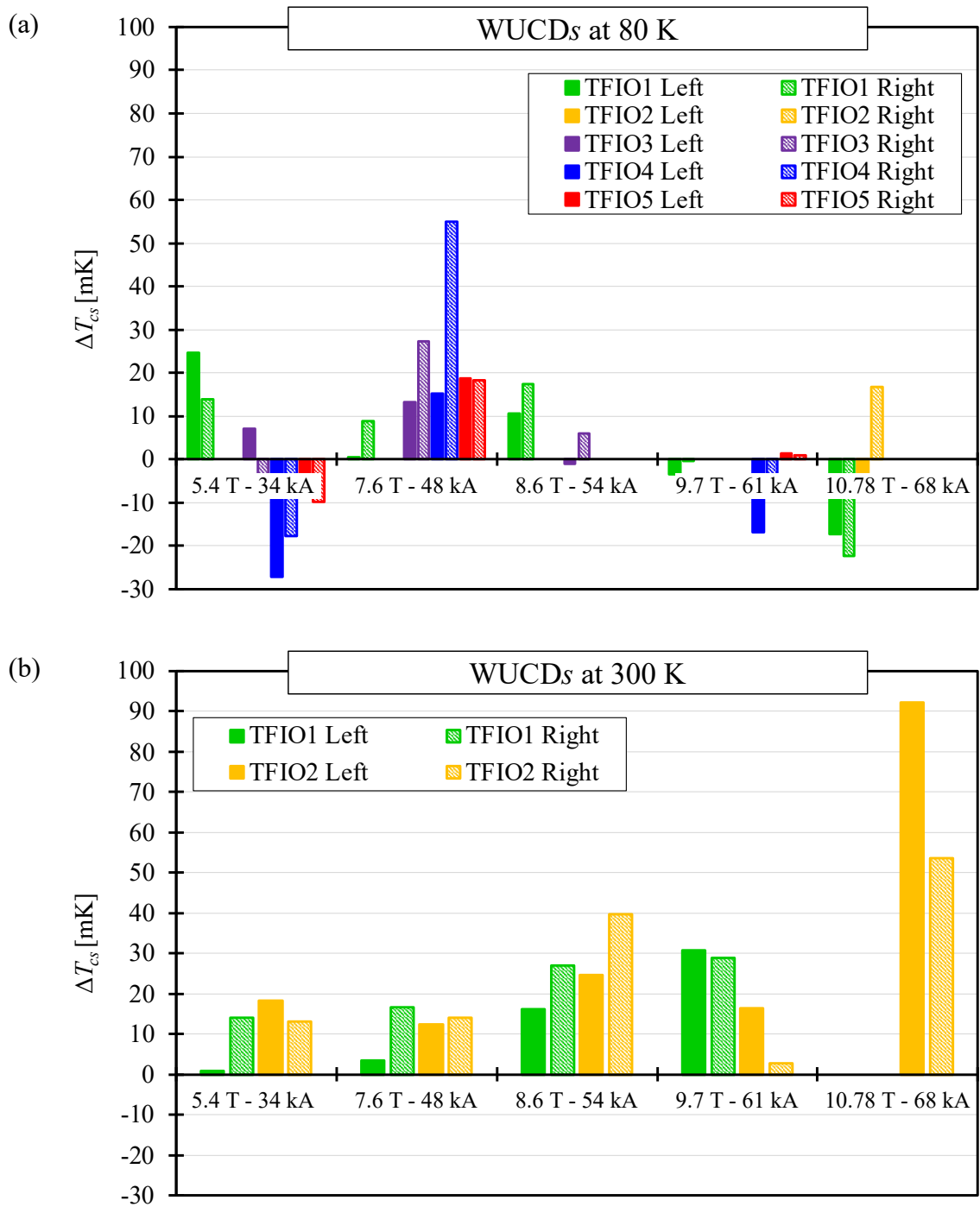
Figure 8. *Drop of T_{cs} at various working conditions for the warm-up cool- down (WUCDs) to (a)* 80 K *and (b)* 300 K.
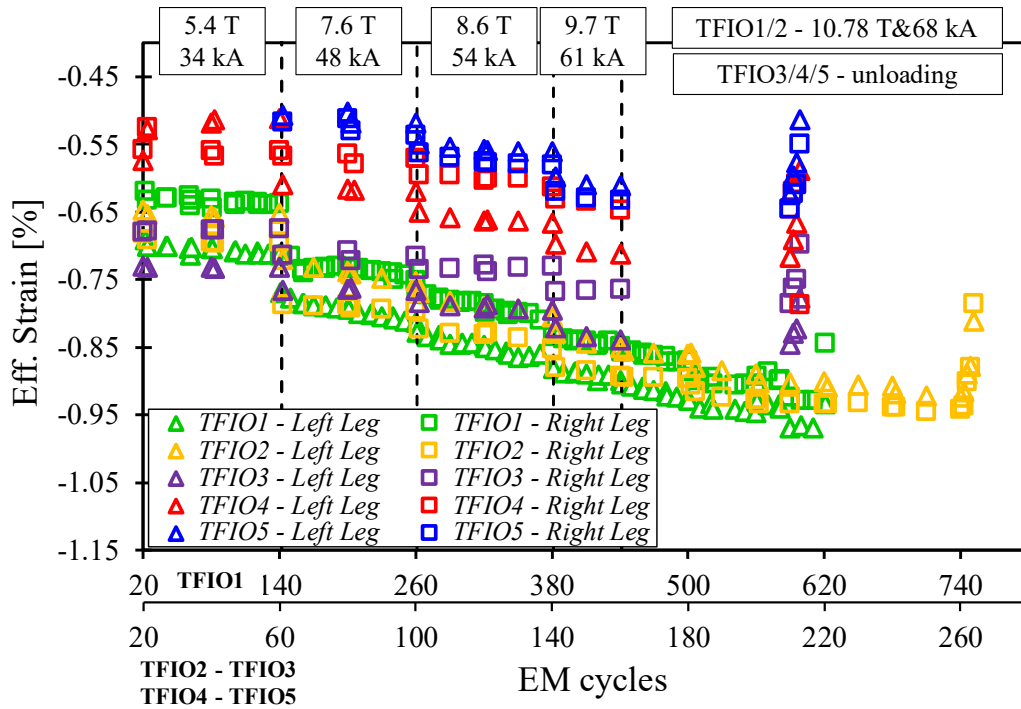
Figure 9. *Effective Strain of the TFIOXX conductors as a function of the number of EM cycles (to be noted that WUCDs are also performed during the tests).*
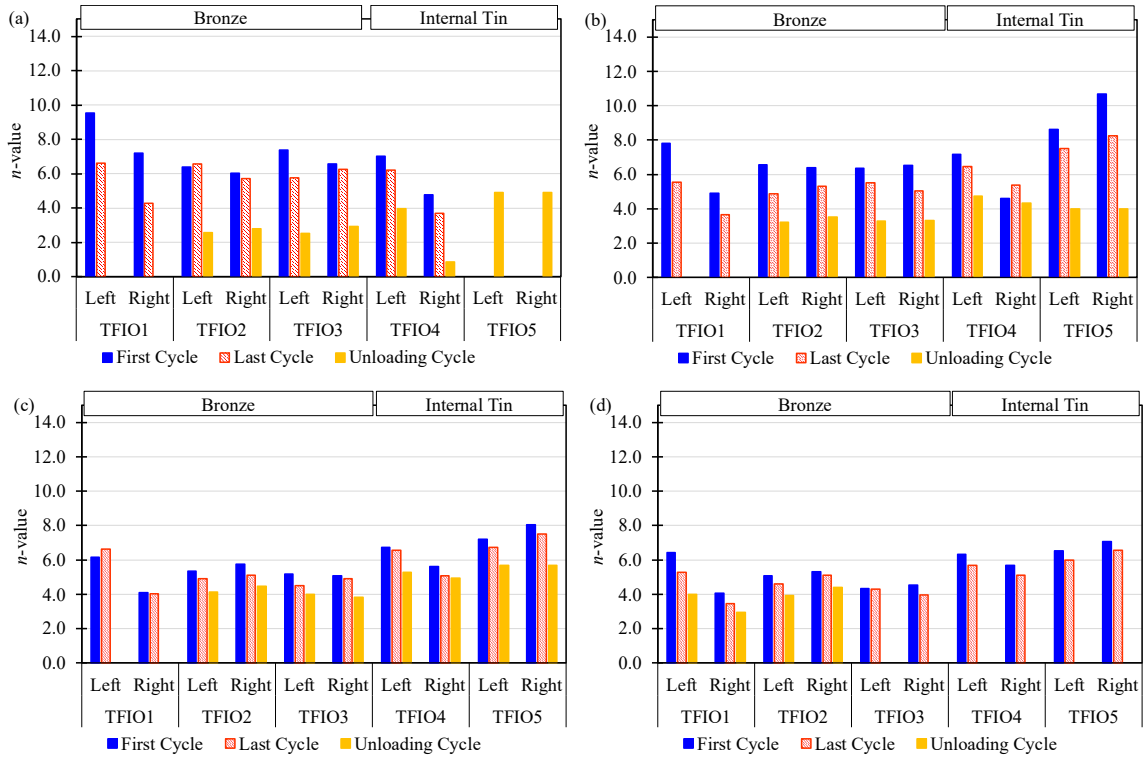
Figure 10. *Effective Strain of the TFIOXX conductors at the following working conditions: (a) 5.4 T - 34 kA, (b) 7.6 T - 48 kA, (c) 8.6 T - 54 kA (d) 9.7 T - 61 kA and (e) 10.78 T – 68 kA.*
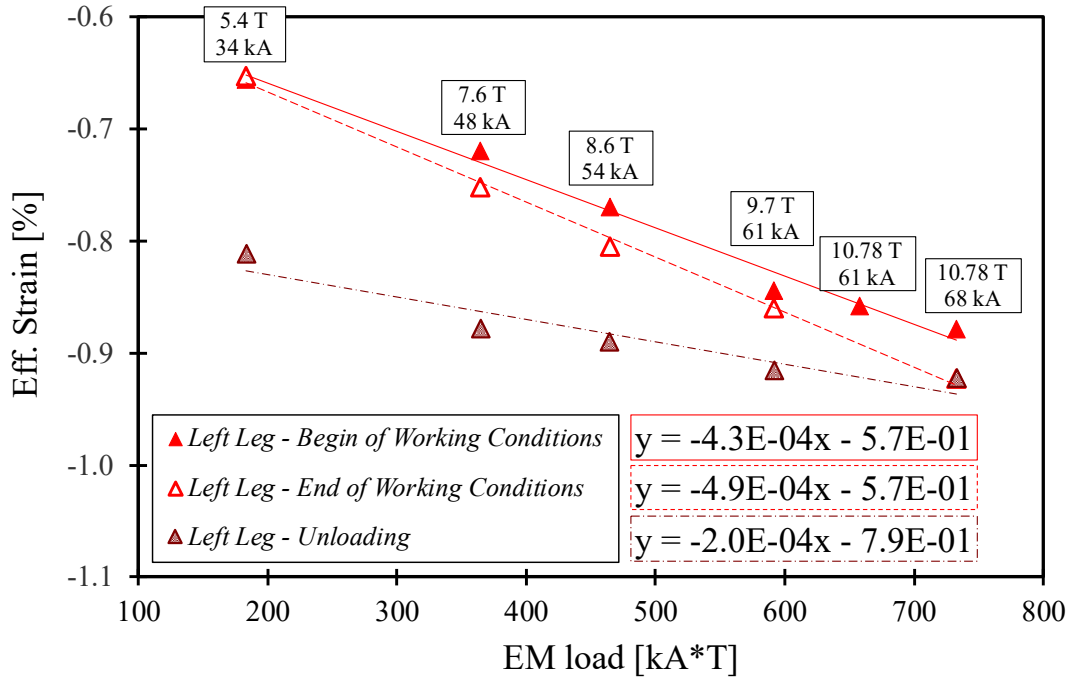
Figure 11. *Effective Strain of the TFIO2 Left Leg as a function of the EM transverse load.*
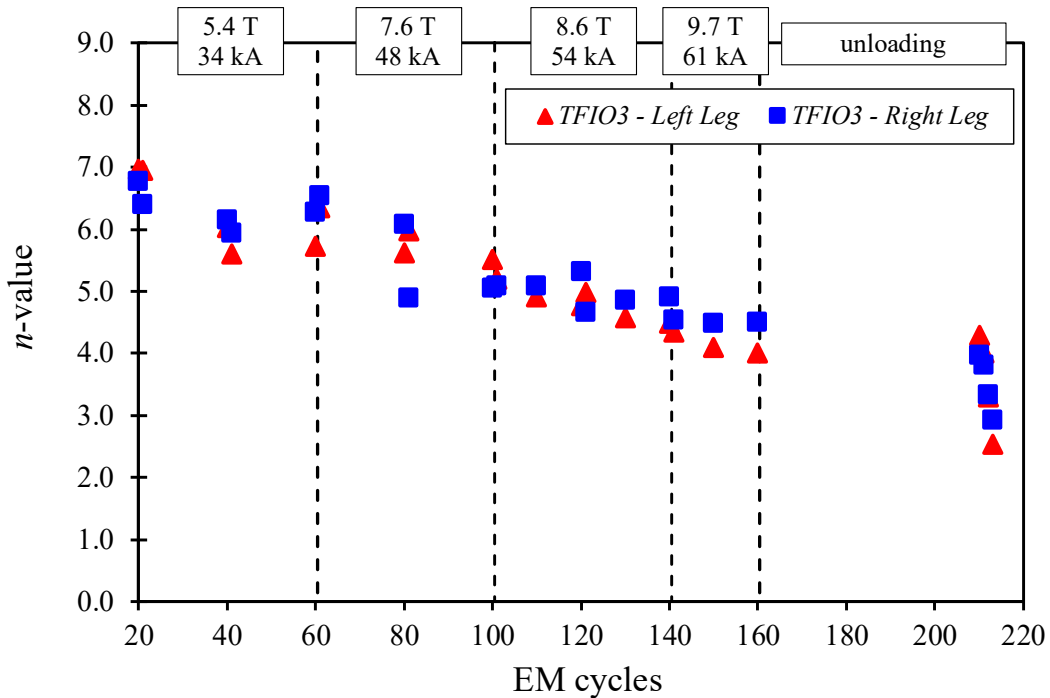
Figure 12. *n-value of the two conductor legs of the TFIO3 sample tested in SULTAN as a function of the number of EM cycles (to be noted that WUCDs are also performed during the tests).*

Figure 13. *n-value of the TFIOXX conductors at the following working conditions: (a)* 5.4 T - 34 kA, *(b)* 7.6 T - 48 kA, *(c)* 8.6 T - 54 kA *(d)* 9.7 T - 61 kA.
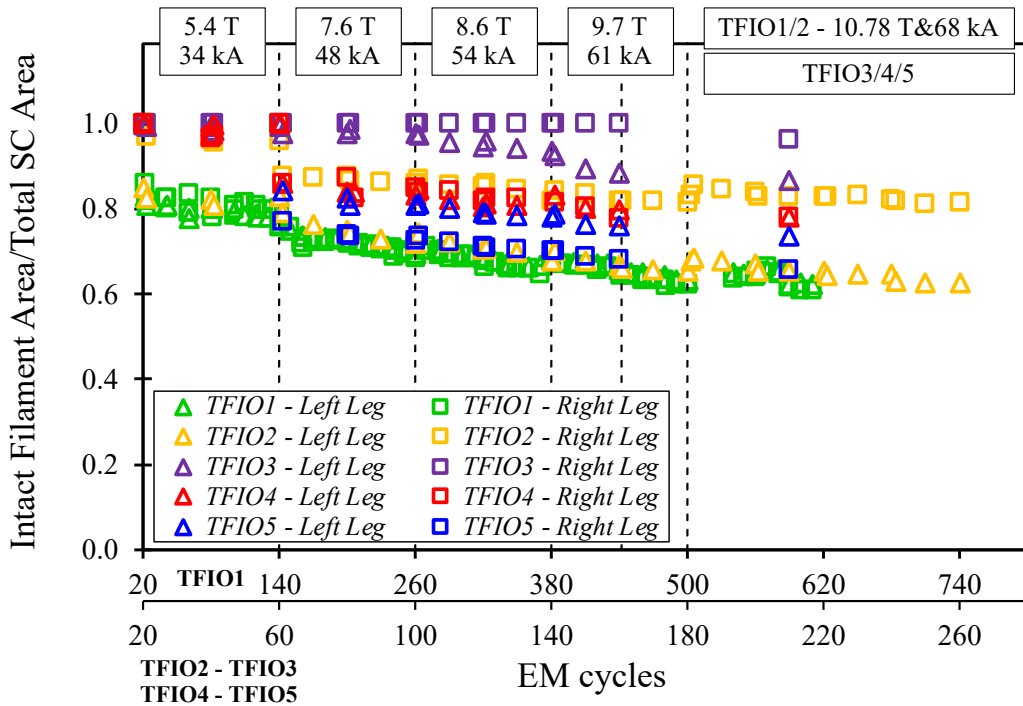
Figure 14. *Evolution during the test campaign of the ratio between the intact filament area and the total superconducting area of the TFIOXX condctors.*
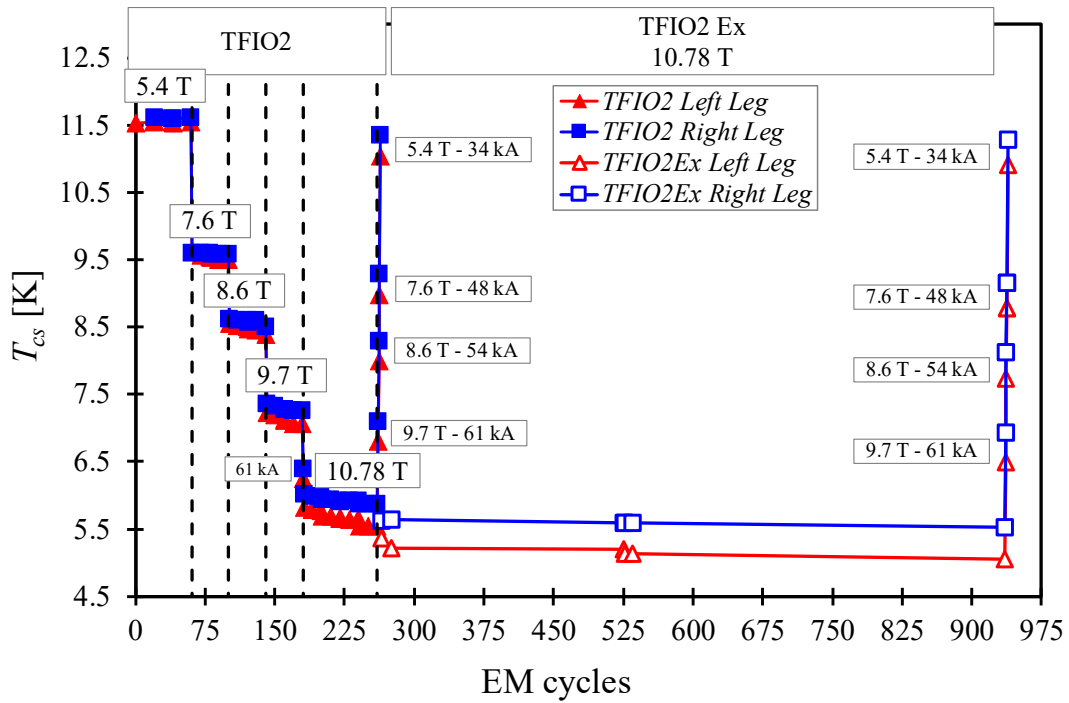
Figure 15. *Voltmetric T_{cs} of the TFIO2 and TFIO2Ex as a function of the number of EM cycles.*
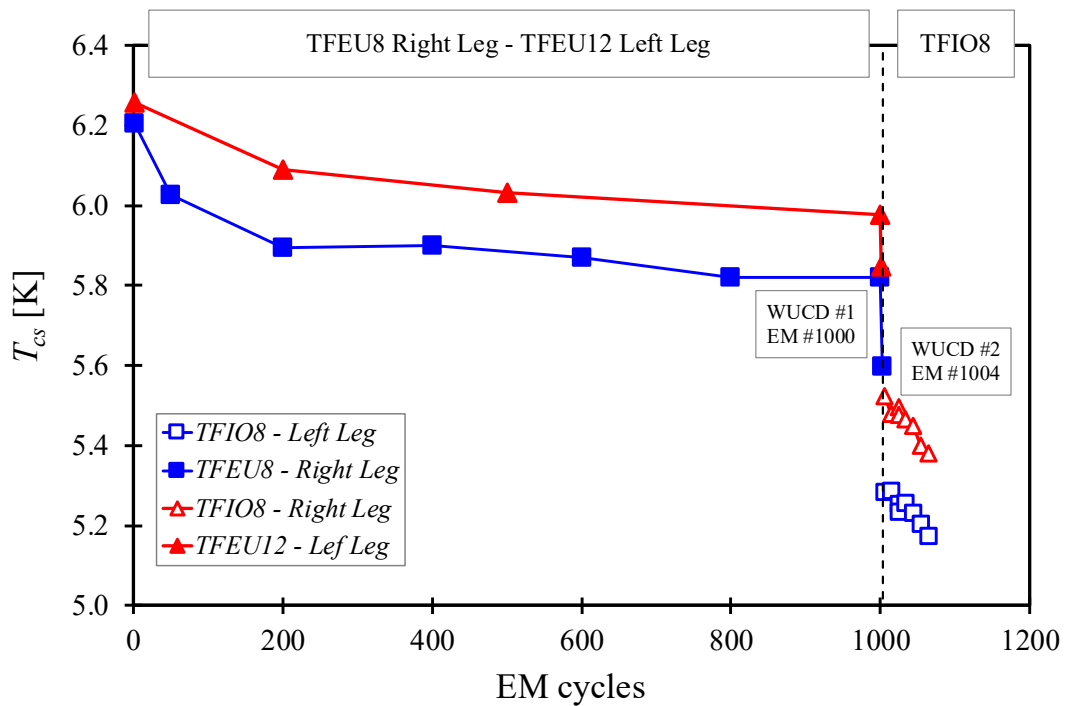

Figure 16. *Voltmetric T_{cs} of the TFIO8, TFEU8 right leg and TFEU12 left leg as a function of the number of EM cycles.*